Solid State Phenomena Vol. 215 (2014) pp 421-426
Online available since 2014/Apr/11 at www.scientific.net

doi:10.4028/www.scientific.net/SSP.215.421

3-D Simulations of Micromagnetic Transition Structures in Vortex Asymmetric Domain Walls

V.V. Zverev[a1],M.N. Dubovik[1,2], B.N. Filippov[1,2]

[1] Ural Federal University, Mira str. 19, Yekaterinburg 620002, Russia

[2] Institute of Metal Physics, UB RAS, S. Kovalevskoy str. 18, Yekaterinburg 620990, Russia

[a]e-mail: vvzverev49@gmail.com

Keywords: magnetic films, micromagnetism, domain walls, Bloch lines, Bloch points

Abstract. The three-dimensional transition structures in the vortex asymmetric domain walls existing in magnetically uniaxial soft magnetic films with in-plane anisotropy are studied by micromagnetic simulations. It is shown that interaction of closely spaced transition structures results in various dynamical scenarios including vortex-antivortex annihilations, creation and annihilation of singular (Bloch) points, and excitation of nonlinear waves.

Introduction

The vortex asymmetric (C-shaped) domain wall in magnetically uniaxial films with in-plane anisotropy was predicted numerically in [1]. This wall is a two-dimensional 180° Bloch-type domain wall with an asymmetrically shifted vortex-like structure in the center.

The asymmetric domain walls exist in four possible orientations [2]. Since all these orientations are energetically equivalent, they have equal likelihood to be observed in real films, possibly in the same wall. The static structures of possible transitions from one wall segment to another (transition micromagnetic structures – TMSs, including special cases of vertical Bloch lines - VBLs) were studied numerically in [3,4]. Kerr magnetooptical domain, domain walls and TMSs observations were reported in [2].

In this work we have studied the magnetization dynamics of closely positioned VBLs. We have shown that transformations of the interacting VBLs may be accompanied by the vortex-antivortex annihilation, the singular (Bloch) point (SP) annihilation and creation. The annihilation process causes a burstlike energy release via spin waves. Similar processes in different nanomagnetic elements were studied in [5,6].

The simulations were performed by solving the Landau-Lifshitz-Gilbert equation using the OOMMF solver [7].

Simulations

We have considered a magnetically uniaxial film with in-plane anisotropy. The values of material parameters are characteristic of Permalloy films of a zero-magnetostriction composition (an exchange constant $A = 10^{-11}$ J/m, an anisotropy constant $K = 10^{2}$ J/m^3, a saturation magnetization $M_s = 800\,\mathrm{G}$, a damping constant $\alpha = 0.01$; the quality factor $Q = K / 4\pi M_s^2$ is small).

We have obtained the equilibrium distributions of the magnetization $\mathbf{M}$ minimizing the sample total energy E:

$$E = \iiint \left(w_{\mathrm{e}} + w_{\mathrm{a}} + w_{\mathrm{m}} \right) d\mathbf{r}, \qquad (1)$$

$$w_{\mathrm{e}} = A\left\{(\partial_x \mathbf{m})^2 + (\partial_y \mathbf{m})^2 + (\partial_z \mathbf{m})^2\right\}, \quad w_{\mathrm{a}} = -K(\mathbf{km})^2, \quad w_{\mathrm{m}} = -\tfrac{1}{2} M_s \mathbf{mH}^{(\mathrm{m})},$$

where $\mathbf{m} = \mathbf{M}/M_{\mathrm{s}}$ and $\mathbf{k}$ is the unit vector directed along axis z. Magnetostatic field $\mathbf{H}^{(\mathrm{m})}$ is determined by solving magnetostatic equations with the corresponding boundary conditions.

For energy minimization we employed the method of conjugate gradients (based on the Fletcher-Reeves algorithm) with discretization on a rectangular grid with a step of 5 nm. A sample has the shape of a parallelepiped with sizes $L_x = 100$ nm (the film thickness), $L_y = 400$ nm (the distance between domains) and $L_z = 750$ nm. The conditions on the domain boundaries read:

$$\mathbf{m}\big|_{y=0} = \mathbf{k}, \qquad \mathbf{m}\big|_{y=L_y} = -\mathbf{k}. \tag{2}$$

The periodic boundary conditions were chosen along the z axis:

$$\mathbf{m}\big|_{z=0} = \mathbf{m}\big|_{z=L_z}. \tag{3}$$

Given these conditions the magnetostatic field calculation is performed according to [8].

To obtain TMSs of specific types, we performed the energy minimization using specially chosen initial conditions. At the first stage, a piecewise constant initial magnetization distribution was chosen to mimic the distribution in a domain wall. Minimizing the energy given by Eq. (1) we find a smooth magnetization distribution corresponding to an asymmetric domain wall. At the second stage, we transform the magnetization in the region $L_z/4 < z < 3L_z/4$ (Ω in Fig. 1a) by one of the three methods shown in Fig. 1d and repeat energy minimization. To form TMSs with given magnetization directions in vortices and antivortices (v and av in Fig. 1b), it is sufficient to introduce to the initial configuration thin layers β with magnetization distributions shown in Fig. 1e. The procedure of energy minimization rapidly smoothes the nonhomogeneity near the cutoff β and leads to formation of a vortex and an antivortex. The direction of $\mathbf{m}$ in the core of the vortex (antivortex) turns out identical to that in the layer β.

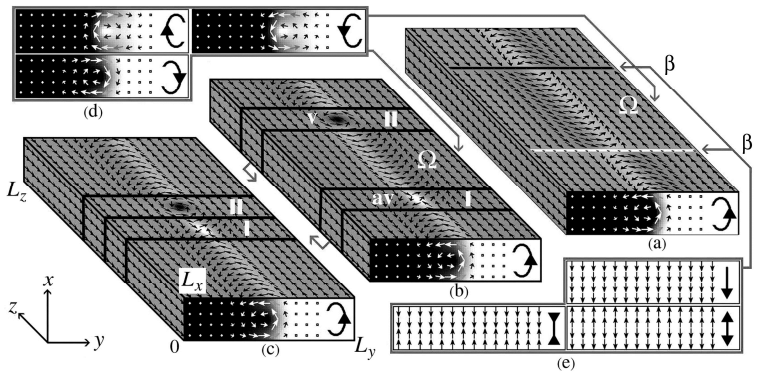

Fig. 1. A magnetization distribution sequence: (a) an initial condition for energy minimization, (b) a segment of the domain wall with minimal energy containing the TMSs I and II, (c) the nonequilibrium configuration with two closely-spaced TMSs. Insets (d), (e) show two-dimensional distributions in the xy-sections of the regions Ω, β, respectively. For every intersection plane the density of gray color is proportional to the projection of the magnetization vector onto the coordinate axis normal to this plane.

In view of the condition (3), the sample shown in Fig. 1b is a closed loop where the TMSs I, II are antipodal. The interaction between these TMSs is weak. In this case the magnetic system is in a stable or well balanced unstable symmetric equilibrium state (it was tested numerically that temporal evolution of this state is very slow).

The nonequilibrium configurations used as initial condition to study the dynamical effects are formed by drawing closer TMS-containing regions I and II using a suitable transformation (transition from the magnetization distribution shown in Fig. 1b to the one in Fig. 1c). The dynamics of magnetization establishment was described using the Landau-Lifshitz-Gilbert equation

$$\frac{d\mathbf{m}}{dt} = -|\gamma|\,\mathbf{m}\times\mathbf{H}_{\text{eff}} + \alpha\,\mathbf{m}\times\frac{d\mathbf{m}}{dt}, \qquad \mathbf{H}_{\text{eff}} = -\frac{\delta E}{\delta \mathbf{M}}, \tag{4}$$

where γ is the gyromagnetic ratio and α is the damping parameter. The equation (4) subject to boundary conditions (2, 3) was solved using the fifth-order Runge-Kutta method on a rectangular grid with a step of 5 nm.

The results of energy minimization and simulation of dynamics are presented in Table 1. The pictograms in the form of open rotationally oriented ovals and vertical arrows represent stylized images of two-dimensional magnetization distributions shown in Fig. 1. Symbols X and Y denote various types of the VBL and the asterisk denotes the Bloch point (SP). Configurations of the magnetization in the VBLs have been described in details in [4]. The sequence of the pictograms read from left to right reflects the order in which TMSs, SPs and domain wall regions are met along the *z* axis in the positive direction (see Fig. 2). Some representative types of ultrafast structural transformations are presented in the right-most column. Here, the energy release and the spin waves generation processes are denoted as "oscill".

Table 1. Configurations of initial distributions, the TMSs obtained by energy minimization and types of ultrafast processes.

Type of structure	Initial distribution	Converging TMSs		Ultrafast processes
		I →	← II	
A	↑ ↓	↑ * ↓	↓ * ↑	no
B	↑ ↓ ↓ ↑	↑ X ↓	↓ X ↑	X X → oscill
C	↑ ↓ ↑ ↓	↑ Y ↑	↓ Y ↓	no
B_1	↑ ↓ ↓ ↓	↑ X ↓	↓ * ↑ X ↓ * ↑	no
C_1	↑ ↓ ↑ ↓	↑ * ↓ X ↑	↓ Y ↓	X Y → * , oscill
C_2	↑ ↓ ↑ ↓	↑ * ↓ X ↑	↓ X ↓ * ↑	X X → oscill
C_3	↑ ↓ ↑	↑ Y ↑	↓ $\bar{Y}$ ↓	Y $\bar{Y}$ → * * → oscill

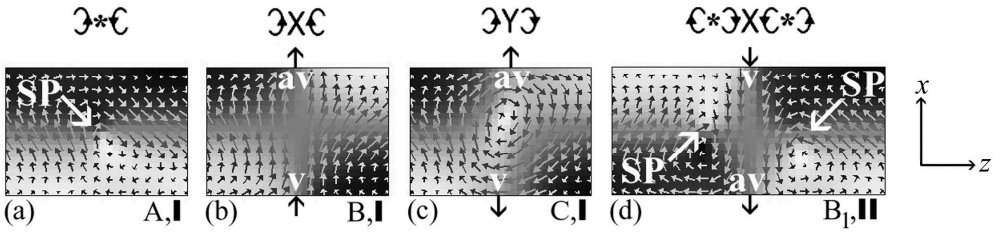

Fig. 2. Sections of the magnetization by the plane $y = L_y/2$. In basic configurations (a) - (c) every TMS is located between the segments of domain walls. The structure (d) is a cluster consisting of X-type VBL and two SPs.

Dynamics of colliding TMSs

Briefly consider the most interesting types of temporal transformations in the domain wall with two neighbouring TMSs.

Cases B and C_2. VBLs of type X annihilate forming a strongly excited domain wall without TMSs. The process is characterized by nearly simultaneous annihilation of two vortex-antivortex pairs located on the opposite sides of the film. The energy release upon annihilation leads to generation of bending oscillations of the wall and spin waves. Due to the imposed boundary conditions, the waves cannot propagate into the domains. For this reason, the model system under consideration behaves as a ring resonator.

Case C_1. In this case the annihilation of a X-VBL and a Y-VBL is observed. The vortex and the antivortex that are located at the surface $x = 100$ nm annihilate generating an additional SP. After time interval $\Delta\tau \approx 0.2$ ns, the second vortex-antivortex annihilation occurs at the surface $x = 0$ nm; in this case, no SP emerges. At the moment of the annihilation the energy release and the spin wave generation are observed.

Case C_3. The Y-type VBL has two modifications Y and $\overline{\mathrm{Y}}$ related via a symmetry transformation. The collision of an Y-type VBL and an $\overline{\mathrm{Y}}$-type VBL occurs as the annihilation of two vortex-antivortex pairs. As the result, two SPs are generated on the opposite boundaries of the film and annihilates inside this film. Every annihilation event is accompanied by the energy release.

3D visualization of vortex, antivortex and SPs trajectories

In the strongly excited medium an accurate investigation of temporal transformations in magnetic films is impeded by the randomly moving magnetization. In this work we localize position vortices, antivortices and SPs using a method based on the numerical calculation of some topological invariants. The trajectories of singular objects constructed by this approach are shown in Fig. 3.

Determining vortex (antivortex) position. The magnetization vectors in cores (centers) of vortices and antivortices are normal to the film boundaries therefore the field of normalized projections of the magnetization vectors on any boundary surface has a singularity in each core point. Define the winding number function

$$j(x,y) = \frac{1}{2\pi} \oint\limits_{\Gamma(x,y)} dt\ \mathbf{i} \cdot \left(\tilde{\mathbf{m}} \times \frac{d\tilde{\mathbf{m}}}{dt} \right), \qquad \tilde{\mathbf{m}} = \mathbf{M}_\perp / |\mathbf{M}_\perp|, \qquad \mathbf{M}_\perp = \mathbf{M} - \mathbf{i}\,(\mathbf{M} \cdot \mathbf{i}).$$

Here $\mathbf{i}$ is a unit vector along the x axis and $\Gamma(x,y)$ is the boundary of the rectangle with the vertices $[x_0,0,0]$, $[x_0,y,0]$, $[x_0,y,z]$, $[x_0,0,z]$, where $x_0 = 0$ and $x_0 = L_x$ are substituted for the lower and the upper boundary surfaces of the film, respectively. If $\bar{y}$ is a coordinate of the vortex (antivortex) center, the plot of $j(y,L_z)$ has a unit jump: $j(\bar{y}+0,L_z) - j(\bar{y}-0,L_z) = \pm 1$. It is convenient to use the function $dj(y,L_z)/dy$ having a delta-like behavior in a vicinity of the point $\bar{y}$. These functions and analogous functions $j(L_y,z)$, $dj(L_y,z)/dz$ allow to find the vortex (antivortex) position $(\bar{x},\bar{y})$ on the boundary surfaces.

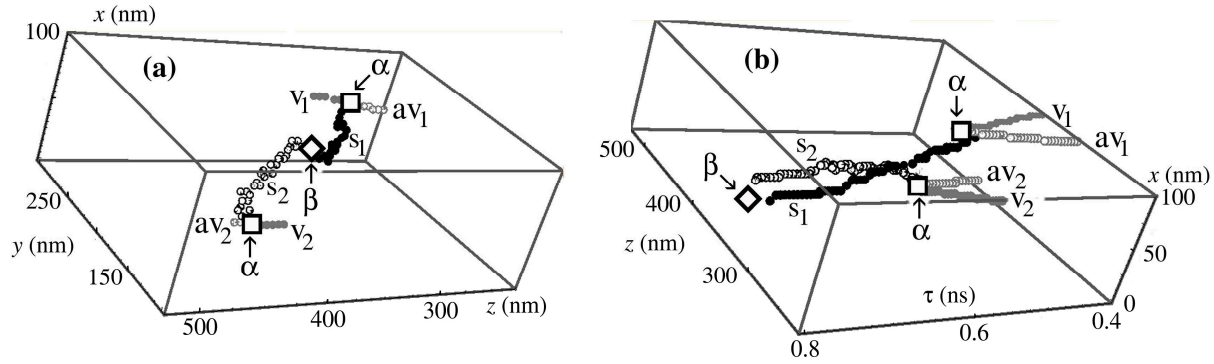

Fig. 3. (a) Trajectories of vortices (v_1, v_2), antivortices (av_1, av_2) and SPs (s_1, s_2) in the solid magnet (the case C_3). The annihilations in vortex-antivortex pairs at the points α result in the generation of SPs. After a small time interval these SPs annihilate at the point β. (b) The same trajectories are shown in the space-time coordinates.

Determining SPs positions. Define the homotopic number χ (topological charge) [9] as a function of coordinates:

$$\chi(x,y,z)=\frac{1}{4\pi}\oint_{S(x,y,z)}\mathbf{g}(\mathbf{r})d\mathbf{s}\,,\qquad \mathbf{g}(\mathbf{r})=\frac{1}{2}\sum_{ijk}\varepsilon_{ijk}m_i(\nabla m_j\times\nabla m_k)=\frac{1}{m_\gamma}\nabla m_\alpha\times\nabla m_\beta\ .$$

Here ε_{ijk} is the Levi-Civita symbol, $\mathbf{g}(\mathbf{r})$ is the gyrocoupling vector and the substitution $(\alpha,\beta,\gamma)=(x,y,z)$ (or (y,z,x), or (z,x,y)) is assumed to take place. Let $S(x,y,z)$ be the boundary surface of the parallelepiped $V(x,y,z)=\{(x',y',z'),0<x'<x,0<y'<y,0<z'<z\}$. Having a sample with SPs and calculating the homotopic number numerically, we detect a jump of ±1 on the $\chi(x,L_y,L_z)$ curve and delta-like peak in the $d\chi(x,L_y,L_z)/dx$ curve at $x=\bar{x}$, where $\bar{x}$ is the SP coordinate. These and similar relations allow determination of the SP position in the three-dimensional space.

Spin waves generation

Spin wave radiation accompanies the structural transformations of the magnetization. Thus to gain a better understanding of dynamics it is essential to correlate wave processes with motion of vortices, antivortices and SPs.

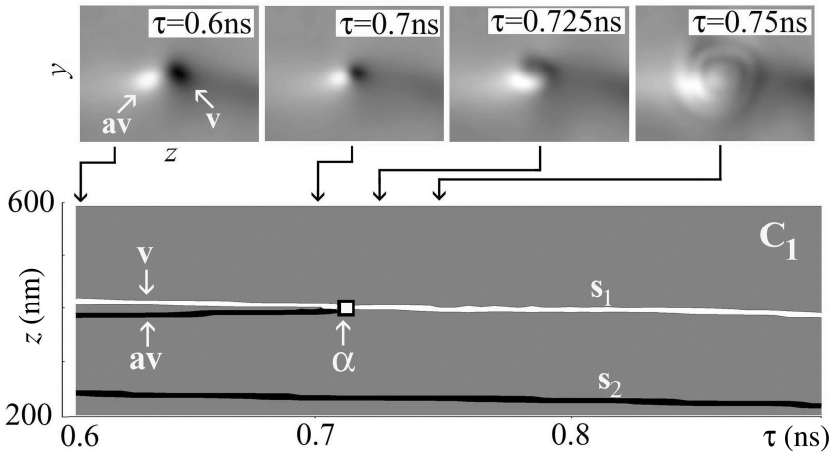

Fig. 4. Case C_1. Four snapshots in upper row display m_x distributions on the surface $x=100$ nm. It is apparent that the vortex-antivortex annihilation gives rise to a ring waves radiation process.

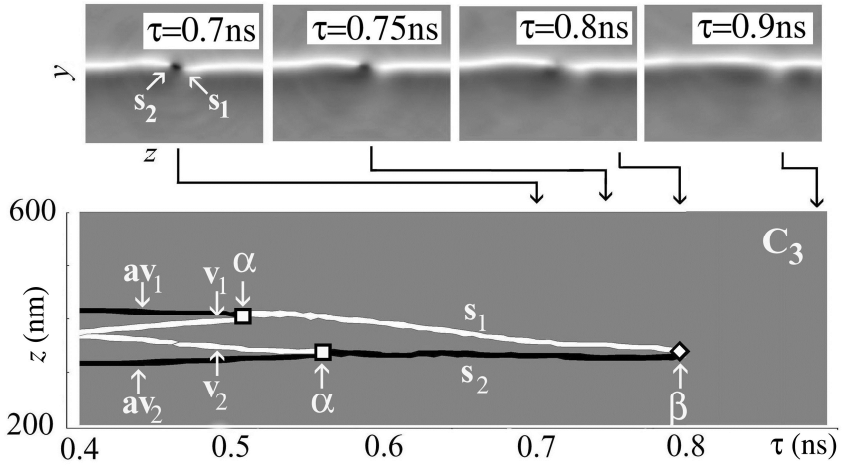

Fig. 5. Case C_3. Four snapshots in upper row display m_x distributions in the medial section $x = 50$ nm. The SPs annihilation produces a solitary wave moving to the right along the domain wall.

Conclusion

We study transition processes in nonequilibrium micromagnetic structures representing regions of various types of asymmetrical vortex domain walls with closely spaced transition structural elements, including vertical Bloch lines (VBLs), singular points (SPs), and clusters consisting of VBLs and SPs, using three-dimensional numerical simulation of the magnetization dynamics. We show existence of various scenarios of dynamic behavior, including the annihilation of transition elements accompanied by the energy release and the initiation of wave processes. We developed a method to analyze micromagnetic structures containing singular objects (vortices, antivortices, SPs) based on calculation of topological invariants.

Acknowledgements

This work was supported by the Russian Foundation for Basic Research (project no. 11-02-00931) and the Department of the Physical Sciences of the Russian Academy of Sciences (program no. 12-T-2-1007).

References

[1] A.E. LaBonte, J. Appl. Phys. 40 (1969) 2450; A. Hubert. Phys. Stat. Sol. 32 (1969) 519.

[2] R. Schäfer, W.H. Ho, J. Yamasaki, *et al*., IEEE Trans. Magn. 27 (1991) 3678.

[3] M. Redjdal, A. Kakay, M.F. Ruane, *et al*., J. Appl. Phys. 91 (2002) 8278.

[4] V.V. Zverev, B.N. Filippov, J. Exp. Theor. Phys. 117 (2013) 108.

[5] R. Hertel, C.M. Schneider, Phys. Rev. Lett. 97 (2006) 177202.

[6] R. Hertel, S. Glida, M. Fähnle *et al*., Phys. Rev. Lett. 98 (2007) 117201.

[7] M. J. Donahue, D. G. Porter, OOMMF User's Guide, Version 1.0 NISTIR 6376, National institute of standards and technology, Gaithersburg, (1999).

[8] K. M. Lebecki, M. J. Donahue, M. W. Gutowski, J. Phys. D 41 (2008) 175005.

[9] A. Malozemoff and J. Slonczewski, Magnetic Domain Walls in Bubble Materials, Academic Press. New York, 1979.

Trends in Magnetism: Nanomagnetism (EASTMAG-2013)
10.4028/www.scientific.net/SSP.215

3-D Simulations of Micromagnetic Transition Structures in Vortex Asymmetric Domain Walls
10.4028/www.scientific.net/SSP.215.421